Stem Cell Reports, Volume *11*

Supplemental Information

Development of a Human iPSC Cardiomyocyte-Based Scoring System for Cardiac Hazard Identification in Early Drug Safety De-risking

Ivan Kopljar, Hua Rong Lu, Karel Van Ammel, Martin Otava, Fetene Tekle, Ard Teisman, and David J. Gallacher

Supplemental Figures

Figure S1

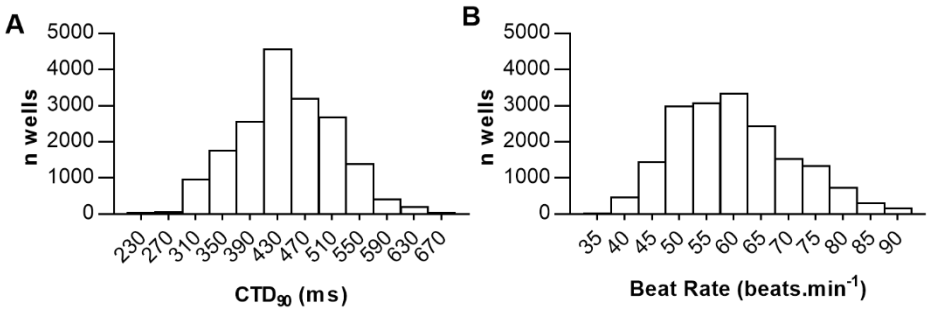

Figure S1. **Beating properties of hiPSC-CMs. Related to Figure 2.** Histograms reflecting a Gaussian distribution of baseline beating properties (CTD_{90} and BR). Data is based on n = 23,183 independent experiments used within the entire analysis that have passed the quality control criteria.

Figure S2

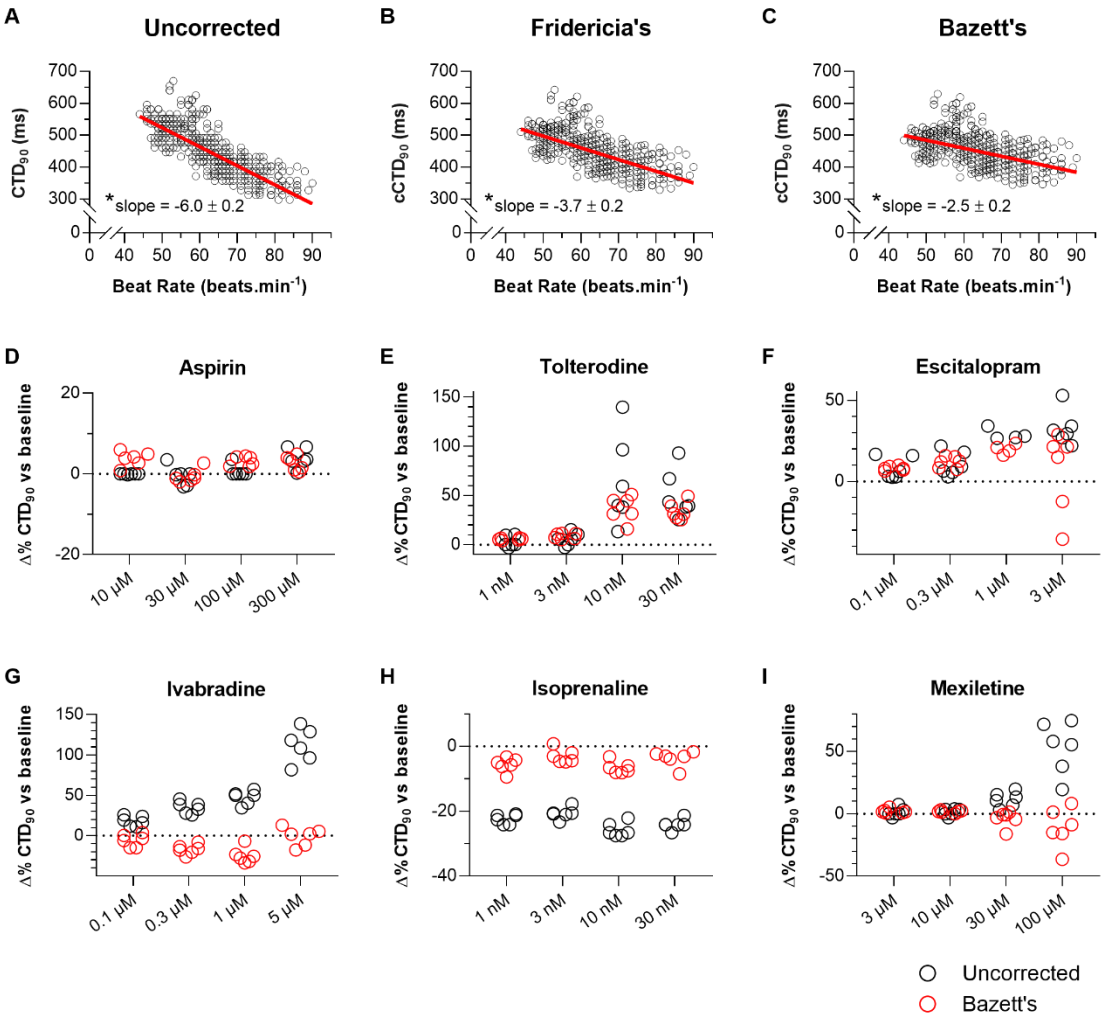

Figure S2. **Correction of CTD_{90} in spontaneously beating hiPS-CMs. Related to Figure 2.** A) Relationship between CTD_{90} and BR using uncorrected baseline experiments, fitted with a linear regression (red line). Correction of CTD_{90} values from A) using B) Fridericia's and C) Bazett's correction formulas still displays a correlation between corrected (c)CTD_{90} and BR. n = 728. Slope is represented as best-fit value ± S.E.M. *: significant deviation from zero; p<0001. D-I) Examples of drug-related Δ% changes for Bazett-corrected compared to uncorrected CTD_{90} values. n = 6 independent experiments. Note for certain drugs strong (directional) differences between uncorrected and corrected data points.

Figure S3

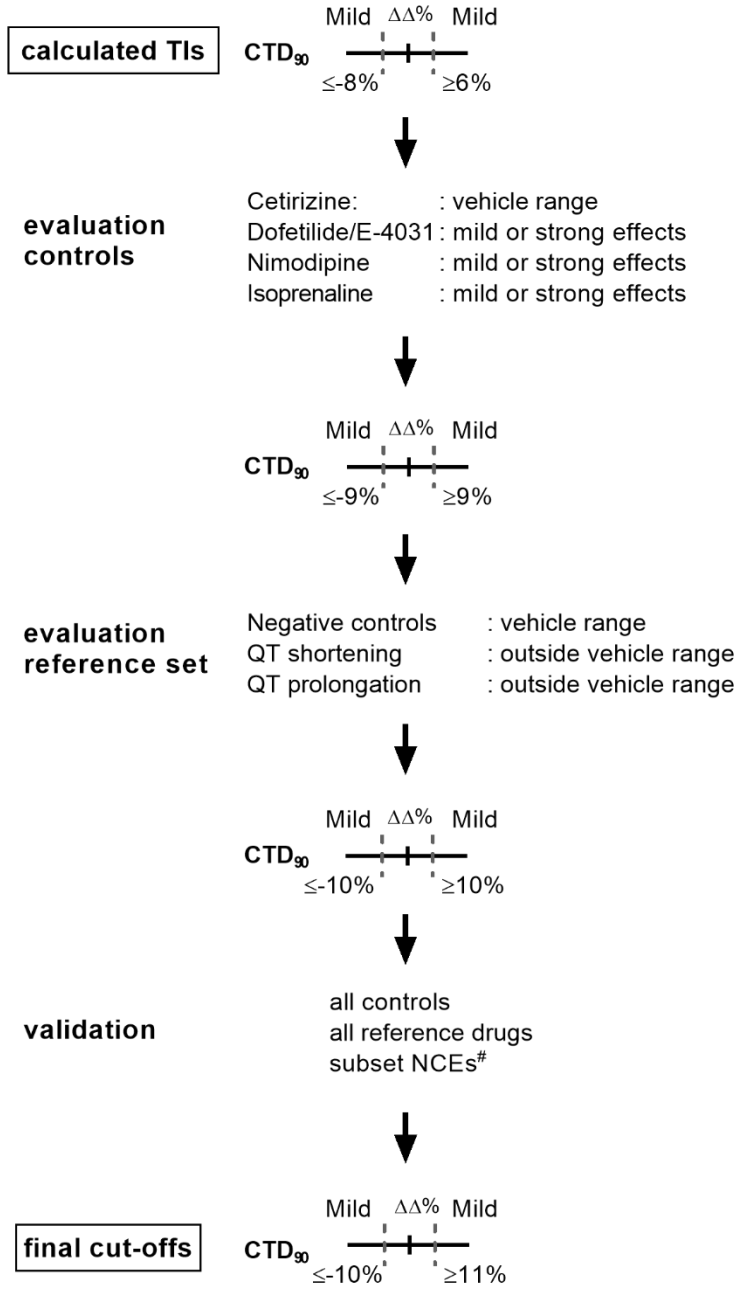

Figure S3. **Optimization of mild CTD_{90} cut-offs. Related to Figure 4.** Process of optimization of mild changes in CTD_{90} starting from calculated TIs. #A subset of NCEs was used to evaluate possible false positive hazard labeling in NCEs. Based on the validation step, the cut-off for CTD_{90} prolongation was set to 11%. This was considered the cut-off where false positives are minimalized whereas the sensitivity for true positive signals is still sufficient.

Figure S4

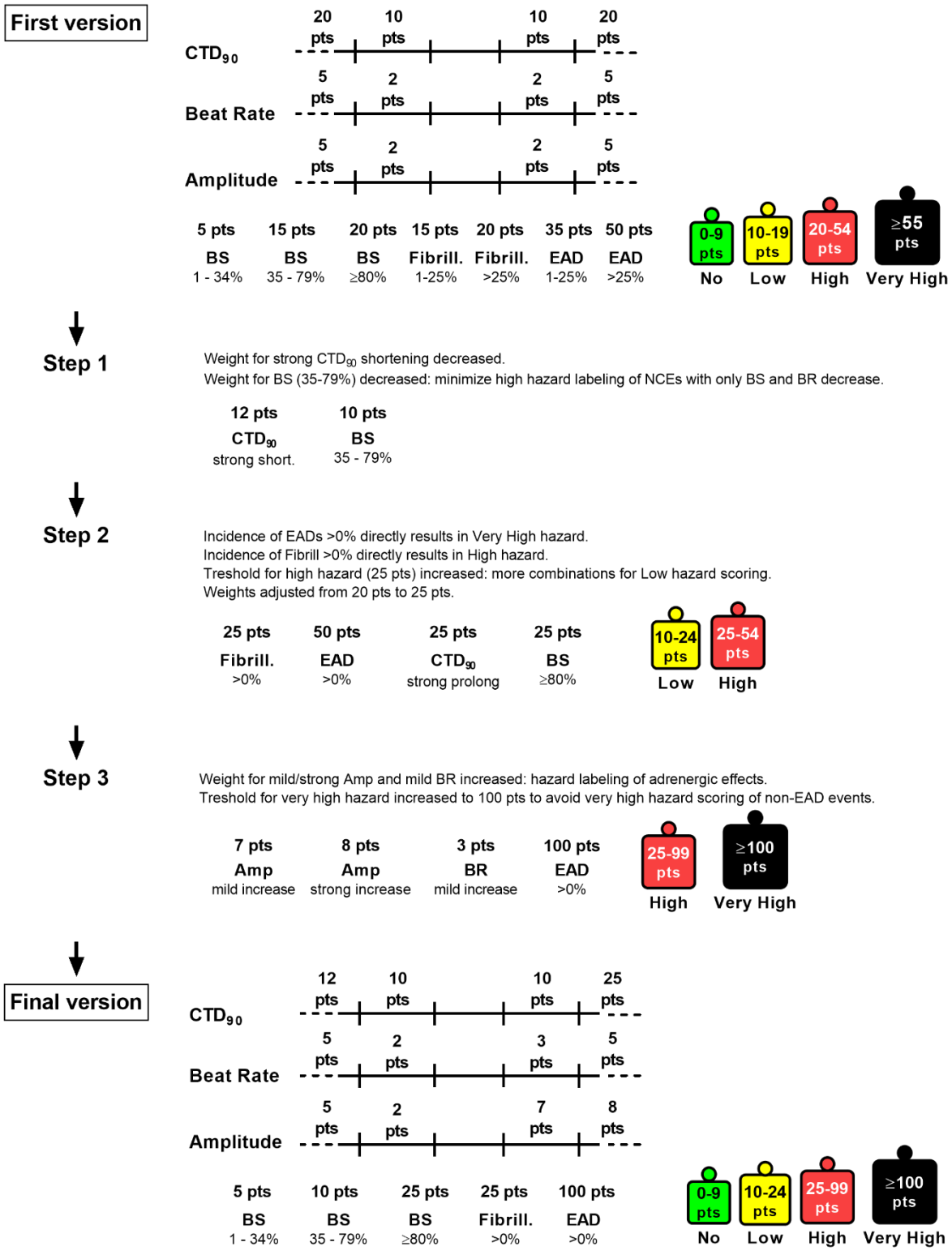

Figure S4. **Optimization of the scoring matrix. Related to Figure 4.** Process of optimization of the weights and hazard labels.

Figure S5

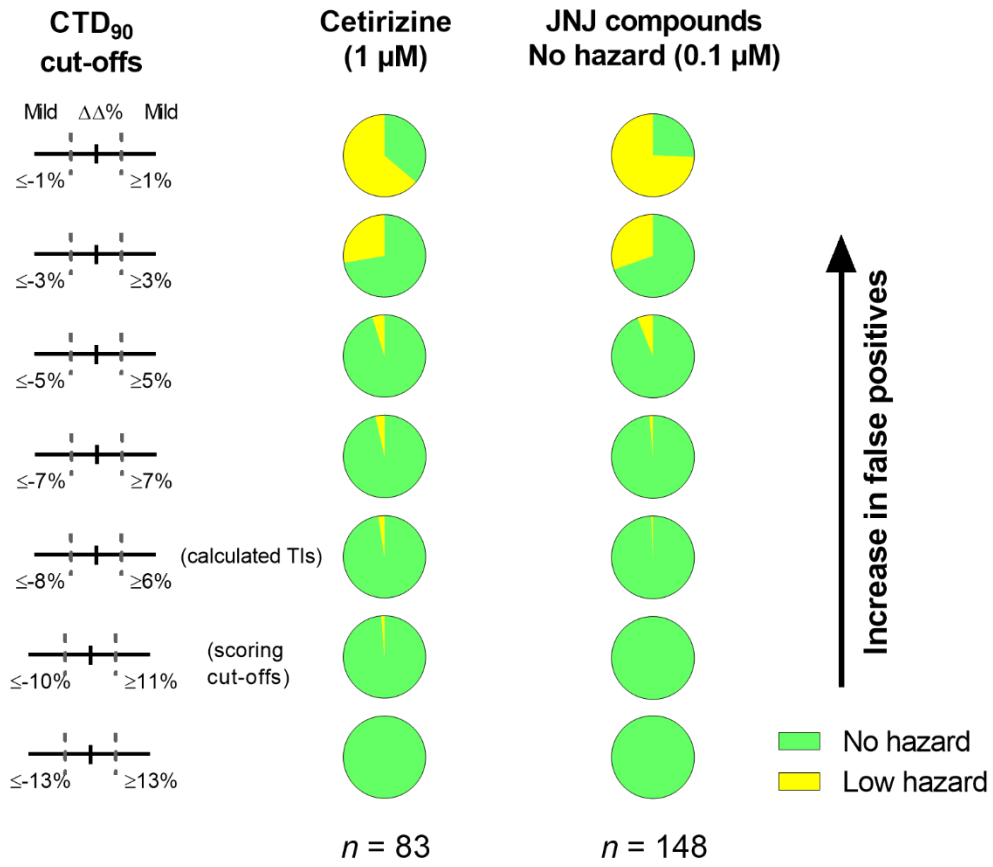

Figure S5. **The effect of CTD_{90} cut-off selection on false positive hazard labeling. Related to Figure 4.** Different cut-offs shown as ΔΔ% changes were evaluated on the negative control cetirizine (1 µM) and on Janssen's NCEs (0.1 µM) which showed an overall no hazard profile within the tested concentration range (0.1–5 µM).

Figure S6

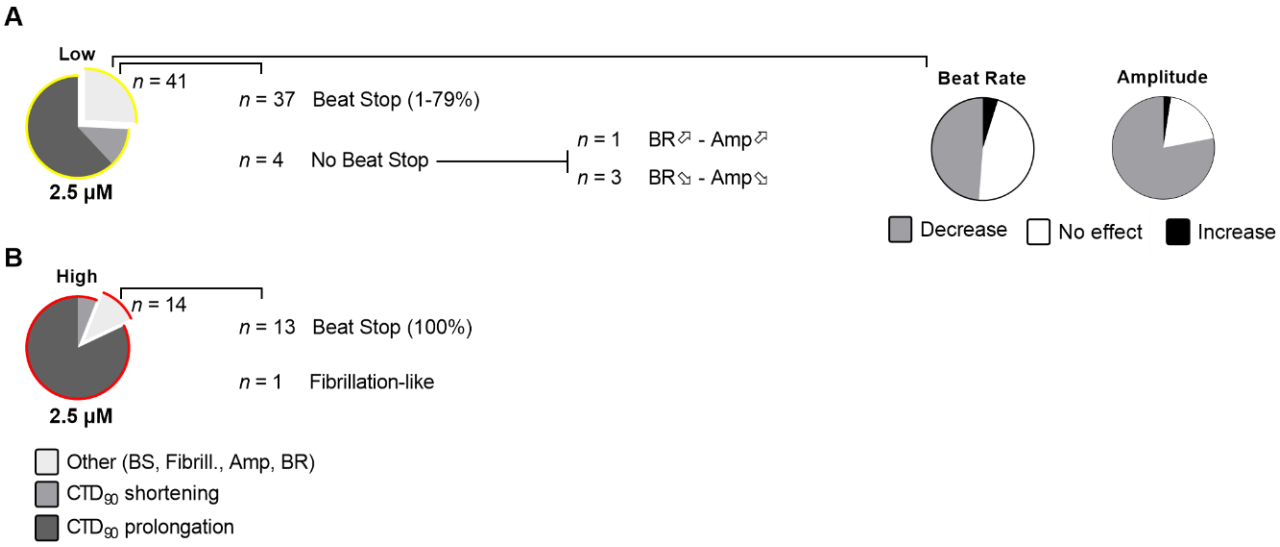

Figure S6. **The impact of non-CTD$_{90}$ parameters on hazard labeling of NCEs. Related to Figure 7.** Detailed analysis of A) low and B) high hazard labeling of NCEs (2.5µM) not related to CTD$_{90}$ changes. n indicates the number of evaluated NCEs.

Figure S7

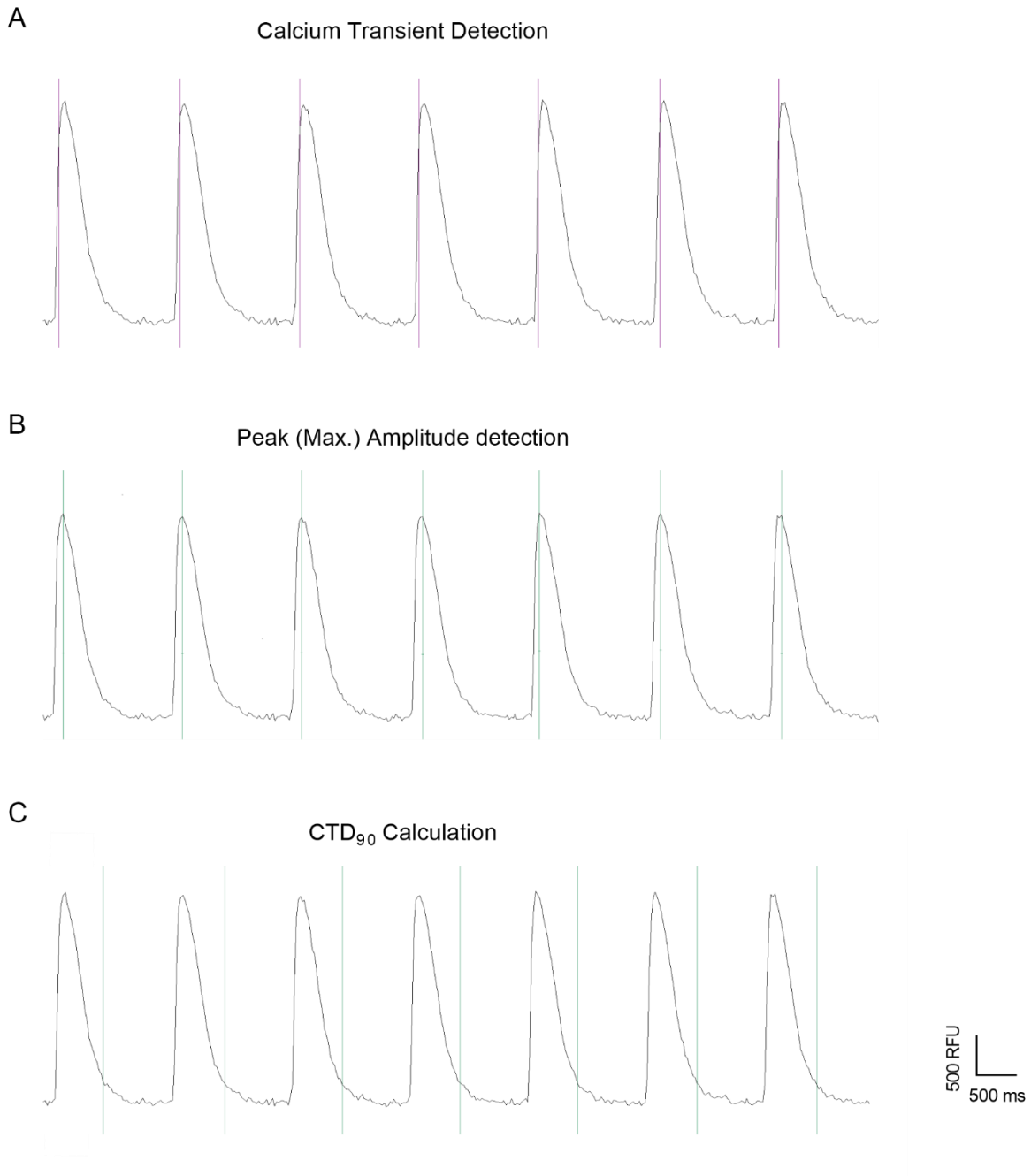

Figure S7. **Calcium transient detection algorithm. Related to Figure 2.** A) Beat/cycle detection. B) Peak amplitude detection. C) CTD_{90} detection/calculation.

Table S1

Compound	Vendor	Product nr.	Lot nr.	Reference free Cmax
Adenosine	Sigma-Aldrich	D9434	SLBH3471V	not available
Ajmaline	Janssen Research Foundation	not available	not available	Redfern et al. (2003)
Alfuzosin	Sigma-Aldrich	A0232	072M4744V	Schulz et al. (2012)
Aprindine	Sigma-Aldrich	A7606	038K4711V	Harmer et al. (2011)
Aspirin	Sigma-Aldrich	A5376	SLBN2916V	Yao et al. (2008)
Atenolol	Sigma-Aldrich	A7655	BCBR3720V	Schulz et al. (2012)
BaCl2	Sigma-Aldrich	342920	MKBH4234V	not available
BAYK8644	WuXi AppTec	EO7563_3_001	not available	not available
Captopril	Sigma-Aldrich	C4042	BCBP9930V	Yao et al. (2008)
Carbachol	Sigma-Aldrich	PHR1511	LRAA3318	not available
Cetirizine	Sigma-Aldrich	C3618	122M4712V	Redfern et al. (2003)
Chlorpheniramine	Sigma-Aldrich	C3025	not available	Ando et al. (2017)
Citalopram	Sigma-Aldrich	PHR1640	LRAA6012	Harmer et al. (2011)
Dextropropoxyphene	Janssen Research Foundation	not available	not available	Schulz et al. (2012)
Digoxin	Sigma-Aldrich	D6003	100M1327V	Schulz et al. (2012)
Dobutamine	Sigma-Aldrich	D0676	055M4018V	Banner et al. (1991)
Dofetilide	TOSLab Ltd.	3979/1	not available	Redfern et al. (2003)
Dofetilide	Sigma-Aldrich	PZ0016	030M4707V	Redfern et al. (2003)
Ebastine	Sigma-Aldrich	E9531	028K4712V	Redfern et al. (2003)
Encainide	Sigma-Aldrich	E9156	018K4611V	Harmer et al. (2011)
Erythromycin	Sigma-Aldrich	E5389	WXBC1653V	Redfern et al. (2003)
Escitalopram	Sequoia Research Products	SRP01460e	not available	Schulz et al. (2012)
Fampridine	ACROS CHIMICA	104570050	A0303988	Schulz et al. (2012)
Flecainide	WuXi AppTec	EO7972_2_002	not available	Ando et al. (2017)
Fluoxetine	Sigma-Aldrich	PHR1394	LRAA9180	Redfern et al. (2003)
Glucose	Sigma-Aldrich	A9251	SLBL0630V	not available
Ibutilide	Sigma-Aldrich	I9910	035M4776V	Redfern et al. (2003)
ICA-105574	WuXi AppTec	EO7972_3_001	not available	not available
Isoprenaline	TCI Chemicals	I0261	YCMCK-JO	not available
Ivabradine	WuXi AppTec	EO7548_6_001	not available	Camm (2006)
JNJ-303	TOCRIS COOKSON	3899	4A/179434	not available
Levcromakalim	Sigma-Aldrich	P154	BGBC4503	not available
Mallotoxin	Sigma-Aldrich	V4629	MKBV4993V	not available
YKP581	SK LIFE SCIENCE	YKP581	BP-01-01-38	not available
Mepyramine	Fluka	PHR1340	LRAA1092	not available
Mesoridazine	Sigma-Aldrich	M4068	081M4705V	Harmer et al. (2011)
Mexiletine	Sigma-Aldrich	M2727	099K1483	Ando et al. (2017)
Mizolastine	Sigma-Aldrich	CDS021588	1582511	Redfern et al. (2003)
Moxifloxacin	Carbosynth Ltd	FM65095	1506016644m	Harmer et al. (2011)
Nicorandil	Sigma-Aldrich	R5648	SLBL9875V	not available
Nifedipine	Sigma-Aldrich	N7634	MKBR1676V	Harmer et al. (2011)
Nimodipine	Prestwick	Prestw-918	not available	Schulz et al. (2012)
Nisoldipine	WuXi AppTec	EO7548_5_001	not available	Schulz et al. (2012)
Olanzapine	Sigma-Aldrich	O1141	035M4781V	Harmer et al. (2011)
Ouabain	Sigma-Aldrich	O3125	021M1512V	not available
Paroxetine	Johnson and Johnson Pharma	not available	not available	Schulz et al. (2012)
Phenytoin	Sigma-Aldrich	PHR1139	P500169	Harmer et al. (2011)
Pinacidil	Sigma-Aldrich	N3539	051M4729V	Thuillez et al. (1991)
Primidone	Sigma-Aldrich	P7295	not available	Schulz et al. (2012)
Procainamide	Sigma-Aldrich	P9391	SLBG4388V	Redfern et al. (2003)

Propafenone	Sigma-Aldrich	P4670	MKBR4240V	Harmer et al. (2011)
Quinidine	Sigma-Aldrich	not available	not available	Redfern et al. (2003)
Raloxifene	Sigma-Aldrich	R1402	MKBS2409V	Czock et al. (2005)
Ranolazine	Sigma-Aldrich	R6152	not available	Ando et al. (2017)
Salbutamol	Sigma-Aldrich	S8260	071M1166V	Schulz et al. (2012)
Sertindole	Sigma-Aldrich	S8072	BGBC4254V	Redfern et al. (2003)
Sertraline	TCI Chemicals	S0507	R8VYD-EC	Harmer et al. (2011)
Sparfloxacin	Sigma-Aldrich	56968	BCBN3519V	Yao et al. (2008)
Tadalafil	Kemprotec	K-1117	not available	Schulz et al. (2012)
Tedisamil	KALI-CHEMIE	KC8857 A5-1/M	not available	Redfern et al. (2003)
Tegaserod	Sigma-Aldrich	SML1504	016M4704V	Appel-Dingemanse et al. (2002)
Thioridazine	Sigma-Aldrich	T9025	BCBQ9396V	Redfern et al. (2003)
Tolterodine	Sigma-Aldrich	PZ0009	100M4706V	Olsson et l. (2001)
Verapamil	WuXi AppTec	EO7972_1_001	not available	Schulz et al. (2012)
Zatebradine	Sigma-Aldrich	Z0127	081M4613V	Roth et al. (1993)
Ziprasidone	USP	1724408	F1J028	Ando et al. (2017)
Zolmitriptan	Sigma-Aldrich	SML0248	022M4724V	Schulz et al. (2012)

Table S1. Compound purchase information and free C_{max} references. Related to Figure 5.

Supplemental Experimental Procedures

Preparation of drug solutions

Compounds were dissolved in dimethyl sulfoxide (DMSO) to obtain a stock solution of 1000-fold the highest test concentration, which was then further diluted to obtain concentrations of 1000-fold the intended concentration. On the day of experiment, these solutions were further diluted with the supplemented Tyrode's solution. Compound addition was done automatically using the Functional Drug Screen System (FDSS/µCell; Hamamatsu, Japan) head stage by adding 100 µL of the 2-fold compound solution to wells with hiPSC-CMs already containing a volume of 100 µL of the experimental solution, finally reaching the intended test concentration in 0.1% DMSO.

Calcium transient detection algorithm

The analysis algorithm consists mainly of multiple parts (beat/cycle, feature and parameter detection) that are executed sequentially. The first part is a beat/cycle detection algorithm using filtering and auto thresholding techniques. The feature detection algorithm then identifies for each detected beat/cycle the beginning (e.g. minimum) and the top (e.g. maximum) of the calcium transient. The third part is a parameter calculation algorithm which uses the detected features to calculate the amplitude and CTD_{90}. Beat rate is calculated based on the time interval between different calcium transient peaks (max.).

Process of defining the weighted points

Defining of the weighted points was based on certain criteria that should reflect the expected hazard labeling for certain drug classes. Here, we explain the most important criteria (requirements) that we applied to design the weighted points system through an iterative approach. The weighted algorithm was first evaluated on the control drugs (Fig. 4C), followed by validation and further fine-tuning using the 66 reference drugs. The first requirement was to have a unique labeling of tested concentrations where EADs were observed (very high hazard). As such, EADs were given 100 points, whereas the cumulation of all other combinations could never reach the 100 points minimum required for very high hazard labeling.

The next requirement was to account for drug responses which would be considered as high hazard. Strong CTD_{90} prolongations (based on dofetilide and E-4031) which could potentially lead to EADs were given 25 points, which was also the minimal number of points required to receive the high hazard label. Mild CTD_{90} prolongations, which also showed clear changes in BR and Amp together with a certain incidence (35-80%) of BS, were also expected to be identified as high hazard. In case all (or most) of the wells showed BS, there would be no primary parameter data available and therefore a high incidence of BS (>80%) was scored as 25 points to reflect the high hazard of this type of response. Also CTD_{90} shortening in combination with changes in BR, Amp and a certain incidence of BS received high hazard labeling. Furthermore, CTD_{90} shortening in combination with strong BR increase and Amp increase were weighted to receive a high hazard label, since this phenotype is observed with strong adrenergic stimulation. On the other hand, CTD_{90} shortening in combination with strong BR decrease and Amp decrease were weighted to receive a low hazard labeling (unless additional BS incidence was observed), since this phenotype most likely reflects calcium antagonism, to which hiPSC-CMs are particularly sensitive. Fibrillation-like observations were also directly associated with high hazard and therefore given 25 points.

Mild CTD_{90} changes in most cases were expected to be labeled as low hazard. A combination of strong changes in BR and Amp, but without any CTD_{90} changes, were relatively rare but could sometimes be observed with e.g. sodium channel blockers. Therefore, strong BR and Amp changes were weighted to reach an accumulated minimum of 10 points (low hazard). Mild decreases in BR and/or Amp were not identified as a hazard. A combination of mild Amp and BR increase was considered an indication of an adrenergic stimulation and therefore labeled as low hazard.

Tolerance interval calculations

Non-parametric tolerance intervals (TIs) were calculated with Wilks' approach (Wilks, 1941) at 95% confidence level covering 90% of population (more details are provided in Supplemental Information). Non-parametric approach truncates number of the lowest and the highest observed values to obtain interval bounds. Wilks' approach utilizes beta distribution to determine number of observations to be truncated to achieve specified confidence and coverage levels. Truncation is performed symmetrically based on Wilks' approach (same number truncated for the lowest and the highest values). The calculations presented in Figure 3 were done on a subset of vehicles and control drugs (mainly plates where reference drugs were tested) based on data from individual experiments. It is important to note that for the calculation of TIs that are supposed to characterize an "usual population", the data set needs to represent the expected effects. Hence, individual experiments were excluded when they showed an unexpected response in hiPSC-CMs that could be attributed to external causes. One-sided

TIs were calculated for the positive controls, whereas for vehicles two-sided tolerance intervals were applied. Note that there is certain minimal sample size (*n* of experiments) needed for non-parametric TIs based on Wilks' approach to achieve given confidence of 95% (when population coverage is 90%). For one-sided interval, at least 29 samples are required, while two-sided interval needs 46 samples at minimum (Krishnamoorthy et al, 2009).

Supplemental References

Ando, H., Yoshinaga, T., Yamamoto, W., Asakura, K., Uda, T., Taniguchi, T., Ojima, A., Shinkyo, R., Kikuchi, K., Osada, T., et al., (2017). A new paradigm for drug-induced torsadogenic risk assessment using human iPS cell-derived cardiomyocytes. J. Pharmacol. Toxicol. Methods. 84, 111-127.

Appel-Dingemanse, S., Horowitz, A., Campestrini, J., Osborne, S., McLeod, J., (2002). The pharmacokinetics of the novel promotile drug, tegaserod, are similar in healthy subjects—male and female, elderly and young. Aliment. Pharmacol. Ther. 15 (7), 937-944.

Banner, W., D. Vernon, D., D. Minton, S., Dean, J., (1991). Non-linear dobutamine pharmacokinetics in a pediatric population. Crit. Care Med. 19 (7), 871-873.

Camm, A.J., (2006). How does pure heart rate lowering impact on cardiac tolerability? Eur. Heart J. Suppl. 8 (suppl_D), D9-D15.

Czock, D., Keller, F., Heringa, M., Rasche, F.M., (2005). Raloxifene pharmacokinetics in males with normal and impaired renal function. Br. J. Clin. Pharmacol. 59 (4), 479-482.

Harmer, A.R., Valentin, J.P., Pollard, C.E., (2011). On the relationship between block of the cardiac Na(+) channel and drug-induced prolongation of the QRS complex. Br. J. Pharmacol. 164 (2), 260-273.

Krishnamoorthy K., Mathew T. (2009). Statistical Tolerance Regions: Theory, Applications, and Computation. John Wiley & Sons, Hoboken, New Jersey.

Olsson, B., Szamosi, J., (2001). Multiple Dose Pharmacokinetics of a New Once Daily Extended Release Tolterodine Formulation Versus Immediate Release Tolterodine. Clin. Pharmacokinet. 40 (3), 227-235.

Redfern, W.S., Carlsson, L., Davis, A.S., Lynch, W.G., MacKenzie, I., Palethorpe, S., Siegl, P.K.S., Strang, I., Sullivan, A.T., Wallis, R., et al., (2003). Relationships between preclinical cardiac electrophysiology, clinical QT interval prolongation and torsade de pointes for a broad range of drugs: evidence for a provisional safety margin in drug development. Cardiovasc. Res. 58 (1), 32-45.

Roth, W., Bauer, E., Heinzel, G., Cornelissen, P.J.G., Van Tol, R.G.L., Jonkman, J.H.G., Zuiderwijk, P.B.M., (1993). Zatebradine: Pharmacokinetics of a novel heart-rate-lowering agent after intravenous infusion and oral administration to healthy subjects. J. Pharm. Sci. 82 (1), 99-106.

Schulz, M., Iwersen-Bergmann, S., Andresen, H., Schmoldt, A., (2012). Therapeutic and toxic blood concentrations of nearly 1,000 drugs and other xenobiotics. Crit. Care 16 (4), R136.

Thuillez, C., Pussard, E., Bellissant, E., Richer, C., Kechrid, R., Giudicelli, J.F., (1991). Arterial vasodilating profile and biological effects of pinacidil in healthy volunteers. Br. J. Clin. Pharmacol. 31 (1), 33-39.

Wilks, S.S., (1941). Determination of Sample Sizes for Setting Tolerance Limits. Ann. Math. Statist. 12 (1), 91-96.

Yao, X., Anderson, D.L., Ross, S.A., Lang, D.G., Desai, B.Z., Cooper, D.C., Wheelan, P., McIntyre, M.S., Bergquist, M.L., MacKenzie, K.I., et al., (2008). Predicting QT prolongation in humans during early drug development using hERG inhibition and an anaesthetized guinea-pig model. Br. J. Pharmacol. 154 (7), 1446-1456.